



Water and salt transport properties of zwitterionic polymers film



Lei Ni^a, Jianqiang Meng^{a,*}, Geoffery M. Geise^b, Yufeng Zhang^a, Jin Zhou^a

^a State Key Laboratory of Hollow Fiber Membrane Materials and Processes, Tianjin Polytechnic University, Tianjin 300387, PR China

^b Department of Chemical Engineering, University of Virginia, Charlottesville, VA 22904, USA

ARTICLE INFO

Article history:

Received 22 October 2014

Received in revised form

13 February 2015

Accepted 4 May 2015

Available online 5 June 2015

Keywords:

Water permeability

Salt permeability

Water/salt selectivity

Zwitterionic film

Desalination

ABSTRACT

Two series of crosslinked zwitterionic polymer films were synthesized via UV-photopolymerization of aqueous solution, and the films were prepared using sulfobetaine methacrylate (SBMA) or carboxybetaine methacrylate (CBMA) as the zwitterionic co-monomer and poly(ethylene glycol) diacrylate (PEGDA) as the crosslinker. The water and salt transport properties of the obtained polysulfobetaine methacrylate (PSBMA) and polycarboxybetaine methacrylate (PCBMA) films were studied using permeation and kinetic desorption methods with crosslinked poly(ethylene glycol) acrylate (PEGA) films as a control. Zwitterionic films absorb more water and are more permeable to both water and salt than PEGA films as a result of interactions between the zwitterions, water molecules, and salt ions. The transport properties of PSBMA and PCSMA depend similarly on crosslinking density, and high water and salt permeability correlates with high water uptake. However, the relationship between salt permeability and salt concentration differed between PSBMA and PCBMA. PSBMA behaves like a charged film, and its salt permeability increases with salt concentration while PCBMA shows the opposite trend. Transport properties for both materials are consistent with a trade-off between water permeability and water/salt selectivity. Zwitterionic films exhibit high permeability/low selectivity among polymers reported in the literature. This result suggests that they could be useful as coating materials for membrane fouling control where the anti-fouling properties of the zwitterionic material is more important than water/salt selectivity.

© 2015 Elsevier B.V. All rights reserved.

1. Introduction

Dense polymer films have been widely used in diverse membrane applications for water scarcity alleviation and alternative energy development. These applications include reverse osmosis (RO), forward osmosis (FO), electrodialysis (EDI), pressure retarded osmosis (PRO), reverse electrodialysis (RED) and fuel cells [1–3]. The ion/salt transport properties of these polymer films play a key role determining the separation performance and energy productivity of these applications [3]. The performance of current polymeric materials must be improved to enhance the performance of water purification and energy technologies, and there is an urgent need to better understand fundamental water and salt transport properties of dense polymeric films.

Zwitterions contain both a positively and a negatively charged moiety on the same pendant group, while maintaining overall charge neutrality [4]. Zwitterionic polymers have received growing attention as a new generation of anti-biofouling desalination materials due to favorable resistance to protein adsorption and bacteria attachment [4–8]. Chang et al. used interfacial

polymerization followed by immobilization of zwitterions by crosslinking to prepare an antifouling NF membrane [4]. Zwitterionic monomers were also directly used in interfacial polymerization to prepare a novel zwitterionic NF membrane [7]. Membrane performance and/or antifouling properties were improved considerably due to the incorporation of zwitterionic moieties in the membrane. However, even as zwitterionic polymers are promising materials for use as antifouling coating layers on membrane surfaces or are of interest as desalting layers of thin film composite membranes, the salt transport properties of zwitterionic polymers are not well understood.

Generally, water and salt transport in non-porous polymers can be described by solution-diffusion theory [9–13]. Polymer structure has a strong impact on the water uptake of the material [2,14–18], which subsequently can influence strongly water and salt sorption, diffusion and permeation properties. In addition, many polymers used as membranes for desalination and energy applications have ionizable or charged functional groups on the polymer backbone [2,13,19]. Therefore, it is important to evaluate the impact of charge on transport properties in these films. Charged and uncharged polymers exhibit very different salt and water sorption and diffusion properties [13]. Uncharged polymers, swollen with water and not containing functional groups that can ionize, exhibit water and salt transport properties that follow a

* Corresponding author at. Tel.: +86 22 83955078; fax: +86 22 83955055.

E-mail address: jianqiang.meng@hotmail.com (J. Meng).

simple partitioning mechanism [11,13–16]. Conversely, charged polymers containing fixed charge groups, which are covalently connected to the polymer backbone and can ionize when the polymer is swollen with water [20], exhibit different ion sorption and diffusion behavior compared to that of uncharged polymers [3,13,20–22]. Ion sorption in an uncharged polymer proceeds by a simple partitioning mechanism and its dependence of ion diffusion properties on salt concentration in the external solution is mainly related to osmotic de-swelling. On the other hand, ion sorption in a charged polymer proceeds by both ion exchange and simple partitioning mechanisms and ion diffusion is strongly influenced by electrostatic interactions.

Zwitterionic polymer films have a high charge density of both positive and negative charge groups but are overall charge neutral, so it is not clear whether the water and salt transport properties of zwitterionic polymers are similar to charged or uncharged polymers. To study the impact of zwitterionic groups on water and salt transport properties, we synthesized UV crosslinked films containing sulfobetaine and carboxybetaine groups crosslinked with poly(ethylene glycol) diacrylate (PEGDA) and characterized their salt transport properties. A crosslinked poly(ethylene glycol) acrylate (PEGA) film was prepared and used as a control membrane. The structures of the two zwitterionic co-monomers (sulfobetaine methacrylate, SBMA, and carboxybetaine methacrylate, CBMA) and the neutral co-monomer, poly(ethylene glycol) acrylate (PEGA), are shown in scheme 1. Two zwitterionic polymers, poly(sulfobetaine methacrylate) (PSBMA) and poly(carboxybetaine methacrylate) (PCBMA), and a neutral polymer, poly(ethylene glycol) acrylate (PEGA), were obtained using UV photopolymerization where the crosslinking density of the polymers was tuned by controlling the ratio of co-monomer to PEGDA.

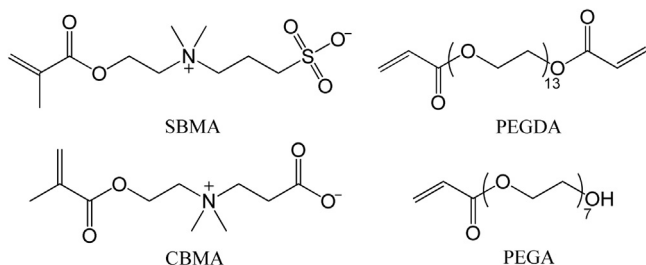
2. Experimental

2.1. Materials and reagents

The photoinitiator 1-hydroxycyclohexyl phenyl ketone (HPK), crosslinker PEGDA ($M_n=700$, $n=13$), co-monomer PEGA ($M_n=380$, $n=7$) and co-monomer SBMA were obtained from Sigma-Aldrich and used as received. The co-monomer CBMA was synthesized according to the method reported in the literature [23] and the purity of the product was confirmed using ^1H NMR (Fig. S1 in Supporting Information). De-ionized (DI) water was obtained from a Millipore MilliQ system (18.2 M Ω cm, 1.2 ppb TOC, pH=6.9). All the other chemicals and reagents were used as received without any purification.

2.2. Film synthesis

Polymer films were prepared by UV induced polymerization of a mixture of zwitterionic monomers, PEGDA crosslinker, HPK photoinitiator and 60 wt% DI water. The pre-polymerization



Scheme 1. Chemical structures of the co-monomers and crosslinker used in the UV crosslinked polymer films.

solution was mixed in an amber glass jar for one hour to completely mix the monomers, crosslinker, and initiator while minimizing exposure to light. Next, DI water was added (60 wt%), and the solution was stirred for an additional hour. N_2 was bubbled through the solution for 10 min prior to polymerization to remove dissolved oxygen. The pre-polymerization solutions with monomer contents of 0, 10, 20, 30, 40, and 50 mol% (molar ratio of co-monomer to PEGDA) were cast between two quartz plates where polytetrafluoroethylene sheets were used as spacers to control the separation between the quartz plates and, thus, the polymer film thickness. The reaction mixture was cured under 312 nm UV radiation for 60 s to produce solid, transparent, cross-linked polymer films. The thickness of the films was measured using a micrometer. The films are designated as PEGAX, PSBMAX and PCBMAX, where X indicates the molar composition of co-monomers in the polymerization mixture.

2.3. Hydrogel film characterization

The surface of each dried polymer film was chemically characterized using ATR-FTIR (Bruker TENSOR37, USA). A ZnS crystal with a 45° angle of incidence was used. The Zeta potential of the films was measured as a function of pH using an Anton-Paar SurPASS Electrokinetic Analyzer with clamping cell apparatus (Anton-Paar GmbH, Austria). All measurements were conducted in an electrolyte solution containing 10 mmol L^{-1} KCl. The pH was varied from 3 to 10, and the temperature was maintained at 298 K. The data were analyzed using the Fairbrother–Mastin algorithm.

2.4. Density and water uptake measurement

The dry film density was measured by Archimedes' principle using an analytical balance (CP 214, Ohaus, USA) with an Ohaus density determination kit. Film density (ρ_p) was calculated as [15,16]

$$\rho_p = \frac{M_A}{M_A - M_L} \rho_0 \quad (1)$$

where M_A is the film mass measured in air, M_L is the film mass measured in a non-solvent (hexane, $\rho=0.659 \text{ g cm}^{-3}$ at 298 K) that does not cause the polymer to swell, and ρ_0 is the density of the non-solvent. Samples were dried overnight under vacuum conditions and at room temperature prior to performing the density measurement.

Equilibrium water uptake at room temperature was determined gravimetrically. Samples were equilibrated in DI water, and the mass of the wet polymer, m_{wet} , was measured after wiping surface water off of the film. Next, the film was dried under vacuum until a constant dry mass, m_{dry} , was obtained and measured. Water uptake was calculated as [15]

$$\text{Water uptake} = \frac{m_{\text{wet}} - m_{\text{dry}}}{m_{\text{dry}}} \quad (2)$$

Assuming volume additivity applies in the cross-linked PEGDA and zwitterionic polymers, the masses measured during the water uptake experiment can be used to determine the volume fraction of water in the fully hydrated film, $V_{\text{H}_2\text{O}}$, and the volume fraction of water is often taken as a measure of K_w , which is the water partition coefficient, or water solubility in the polymer [13,24]:

$$V_{\text{H}_2\text{O}} = \frac{m_{\text{wet}} - m_{\text{dry}}}{\frac{\rho_{\text{H}_2\text{O}}}{\rho_{\text{H}_2\text{O}} + \rho_p} (m_{\text{wet}} - m_{\text{dry}}) + m_{\text{dry}}} = K_w \quad (3)$$

where $\rho_{\text{H}_2\text{O}}$ is the density of water (taken as 1.0 g cm^{-3}).

2.5. Water transport properties

DI water was pressurized above a film sample in a high-pressure dead-end stirred cell (HP4750, Sterlitech Corp., Kent, WA). Permeate volume, V , was measured as a function of time, t , and the hydraulic water permeability was determined as [9,13,17,24]

$$P_w^H = \frac{\Delta V}{\Delta t A \Delta p} \ell \quad (4)$$

where ℓ is the hydrated (wet) film thickness, Δp is the trans-membrane pressure and A is area of the film available for transport. The solution-diffusion mechanism can be used to describe water transport in non-porous polymer films [25]. In this model, an applied pressure difference generates a water concentration gradient across the film. This concentration gradient drives diffusion of water. Fick's law can be used to express water transport in terms of a diffusive permeability P_w , and this permeability is often related to the experimentally determined hydraulic water permeability as [13]

$$P_w = D_w K_w = P_w^H \frac{RT}{V_w} \quad (5)$$

where D_w is the average water diffusion coefficient across the thickness of the film, T is temperature, R is the ideal gas constant, and V_w is molar volume of water ($18 \text{ cm}^3 \text{ mol}^{-1}$). Eq. (5) is only applicable to polymers that do not absorb a significant amount of water, and when this relationship is applied to highly swollen polymer films, the water diffusivity, calculated using Eq. (5) from the hydraulic water permeability and K_w , can appear to exceed the self-diffusion coefficient of water [26]. Paul derived a relationship, applicable to highly swollen polymers, between the hydraulic and diffusive water permeability values based on Fick's Law of diffusion [13,26–28]:

$$P_w = P_w^H \frac{RT}{V_w} \frac{(1 - K_w)}{\delta} \quad (6)$$

where δ is the slope of the water volume fraction versus activity isotherm in the limit where the water activity approaches.

2.6. Salt solubility

Salt transport in the polymer film was characterized using a kinetic desorption technique [16]. First a zwitterionic polymer film was immersed in 50 cm^3 of NaCl solution for 24 h, removed and quickly wiped dry (to remove solution on the surface). The sample was then placed in a beaker containing 50 cm^3 of DI water at 298 K. The beaker was stirred vigorously to ensure complete mixing of the solution, and the beaker was covered with laboratory film to minimize changes in the conductivity of the solution due to evaporation. The conductivity of the solution was measured using a conductivity meter (InoLab 7310, WTW, Germany) and recorded at 5 s intervals at 298 K. The conductivity values were converted to NaCl concentration using a calibration curve, and a Fickian analysis of solute desorption was used to calculate the diffusion coefficient of NaCl in the polymer as [14,16]

$$D_s = \frac{\pi \ell^2}{16} \left[\frac{d(M_t/M_\infty)}{d(t^{1/2})} \right]^2 \quad (7)$$

where ℓ is the average thickness of the hydrated film, M_t is the mass of salt in the solution at time t , and M_∞ represents the total amount of salt desorbed during the course of the experiment. The derivative in Eq. (7) can be determined graphically as it represents the slope of the linear region (i.e., when $M_t/M_\infty < 0.6$) of a plot of M_t/M_∞ versus $t^{1/2}$.

The salt sorption coefficient, K_s , is defined as the ratio of the volumetric concentration of NaCl in the polymer to the concentration of NaCl in the solution used to first equilibrate the polymer (i.e., $\frac{\text{g NaCl/cm}^3 \text{ polymer}}{\text{g NaCl/cm}^3 \text{ solution}}$). The value of K_s can be determined from the total amount of salt desorbed from the polymer, M_∞ , during the kinetic desorption experiment under the assumption that all of the salt that was initially sorbed in the polymer desorbs during the kinetic desorption experiment. The salt permeability coefficient, P_s , can be estimated as the product of the measured diffusion and sorption coefficients according to the solution-diffusion model [14]:

$$P_s = D_s K_s \quad (8)$$

2.7. Salt permeability

NaCl permeability was measured using a jacketed diffusion cell apparatus where the membrane separated two chambers (35 mL PermeGear Side-Bi-Side Diffusion Cell, Hellertown, PA, USA). The solution in each chamber was well mixed by vigorous mechanical stirring. The upstream chamber (donor cell) was filled with a salt solution of specified concentration, and the downstream chamber (receiver cell) initially contained DI water. The receiver cell salt concentration was measured over time using conductivity measurements and a calibration curve. The temperature of the experiment was held constant by circulating water between the jacket of the diffusion cell and an external bath. If the two chambers of the diffusion cell are of equal volume, the salt permeability coefficient, P_s , can be calculated as [14,26]

$$\ln \left[1 - \frac{2C_R[t]}{C_D[0]} \right] = - \left[\frac{2AP_s}{V\ell} \right] t \quad (9)$$

where $C_R[t]$ is the salt concentration in the receiving cell at time t , $C_D[0]$ is the concentration of salt charged to the donor cell, A is the area available for transport, V is the chamber volume, and ℓ is the hydrated sample thickness.

3. Results and discussion

3.1. Synthesis of the zwitterionic films

The synthesis of UV-crosslinked films using PEGDA as a cross-linker have been well documented in literature [16] and sulfobetaine and carboxybetaine are typical zwitterionic co-monomers. Polymer films were synthesized using PEGDA as the crosslinker and using PEGA, SBMA, or CBMA as the co-monomer. Synthesis of the zwitterionic films was first attempted using only the mixture of monomers with HPK. The solid zwitterionic monomers, however, are insoluble in PEGDA. Therefore, 60% water was added to dissolve the zwitterionic monomers and prepare a homogeneous pre-polymerization solution. All of the polymerized films were optically clear and transparent suggesting that the films do not contain pore structures large enough to scatter visible light. They also exhibited favorable mechanical integrity. The chemical composition of the co-monomer and of the surface of the films was analyzed by ATR-FTIR. The ATR-FTIR spectra of SBMA monomer, PEGA film, PSBMA50 film and PCBMA50 film are shown in Fig. 1. Absorption at 1643 cm^{-1} is attributed to the C=C group of the SBMA co-monomer. This band was not observed in the cross-linked film spectra indicating that a negligible amount of unreacted SBMA exists in the crosslinked film. It should be noted that the films had not been soaked in water prior to the ATR analysis. Therefore, we believe that the co-monomer content of the cross-linked film was equal to that of the prepolymerization mixture.

Film density was measured as a function of co-monomer content because polymer density can influence the transport properties of dense polymer films [15,29]. As shown in Fig. 2, the density of SBMA copolymer films increases with the increasing SBMA content, but the density is essentially unchanged for PEGA and CBMA copolymers. The difference in the dependence of polymer density on co-monomer composition for the different films may result from competing contributions of the bulky nature of the pendant groups and their self-associations (attractive intermolecular interactions).

Each co-monomer (i.e., SBMA, CBMA, and PEGA) has a pendant group that is both available for self-association and can disrupt chain packing due to the size of the pendant group. The self-association is mostly aroused by electrostatic interaction between cationic and anionic groups for zwitterions (SBMA and CBMA) while is mostly aroused by hydrogen bonding for PEGA. Increasing co-monomer content leads to an increase in the number of self-associations, and this increase in self-associations could subsequently result in a denser network structure. This interpretation may be particularly applicable to the SBMA films because these materials (compared to the other materials studied) are expected to have very strong electrostatic interactions as sulfonate groups and ammonium groups have similar charge densities [30,31]. For the CBMA and PEGA films, increases in density due to self-associations, which is likely weaker in these materials compared to SBMA, may be offset by chain packing disruptions due to the increase of pendent chains in the polymer [32].

Surface charge properties of PEGA30, PSBMA30 and PCBMA30 films can be determined by measuring streaming potential [28]. The zeta potentials of the three films are presented in Fig. 3 as a

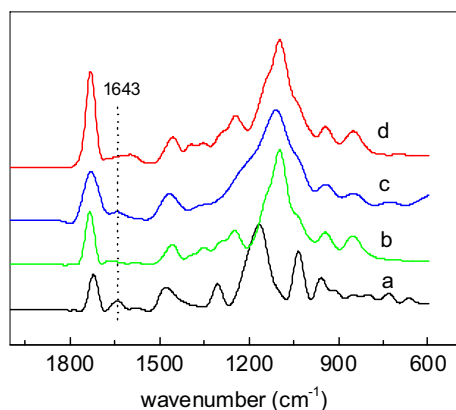


Fig. 1. FTIR spectra of (a) SBMA monomer, (b) PEGDA film, (c) PSBMA film and (d) PCBMA film.

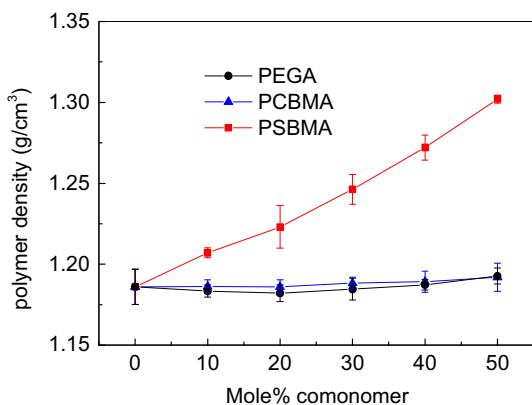


Fig. 2. Density of dry polymer film as a function of the co-monomer content.

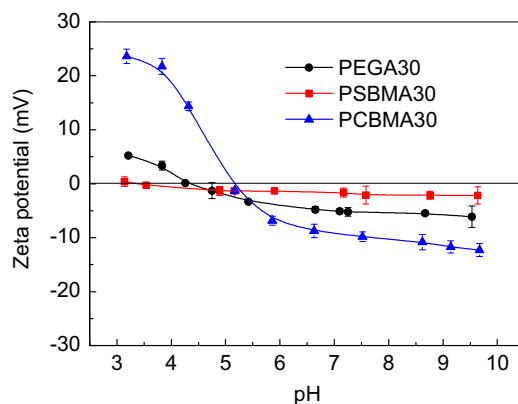


Fig. 3. Zeta potential of the polymer films as a function of pH measured using 10 mmol L^{-1} KCl electrolyte solution.

function of solution pH. The PEGA30 film has small zeta potential, which is slightly positive at a pH below 3 and slightly negative at a pH over 3. We believe this result is due to adsorption of H_3O^+ and OH^- ions via hydrogen bonding [33,34], which is expected because PEGA30 lacks ionizable groups.

The PSBMA30 film exhibits zeta potential values that are nearly zero over the pH range tested, and this behavior may be due to complete ionization of the positive quaternary ammonium group and the negative sulfonate group. On the other hand, PCBMA30 shows typical amphoteric characteristics and is positively charged at acidic pH and negatively charged at alkaline pH. The positive zeta potential values of PCBMA film below pH 4 are relatively high, and this result may be due to ionization of the quaternary ammonium group as the carboxyl groups are expected to be protonated below pH 4. Transport properties of the polymeric films were evaluated at neutral pH, where the Zeta potential of both PSBMA and PCBMA is relatively small.

3.2. Water transport properties

Polymer film water uptake and water volume fractions are presented in Fig. 4(a) and (b), respectively. Water uptake increases with co-monomer content, and this result can be attributed to incorporation of charged groups within the polymer and a decrease in the crosslink density of the films that could lead to enhanced polymer swelling. Fig. 4 also illustrates the influence of co-monomer type on water uptake for films at similar crosslink density. PSBMA films exhibit the highest water uptake, followed by PCBMA and PEGA. We believe the different water binding characteristics of the three monomers can explain this result [35]. The PEG ether groups hydrogen bond with water via the lone pair electrons on the oxygen atoms, and this hydrogen bond strength is less than that for the polymers that contain highly polar charged groups. The sulfonate group is more polar than the carboxylate group, so hydrogen bonding between water and the sulfonate group should be the strongest of the three materials. As a result, water uptake is highest in PSBMA and smallest in PEGA.

Fig. 5 shows the hydraulic water permeability (calculate using Eq. (5)) of the three cross-linked films as a function of co-monomer content and water content. Noted here that the hydrated film thickness range from $110 \mu\text{m}$ to $170 \mu\text{m}$. As shown in Fig. 5(a), the trends of water permeability as a function of the co-monomer content are similar to trends in water sorption. The hydraulic water permeability increases systematically with co-monomer content. The relative values of the water permeability with respect to the co-monomer type is also similar to the order of water uptake, i.e., for a given co-monomer content, water permeability decreases in the order $\text{SBMA} > \text{CBMA} > \text{PEGA}$. We believe

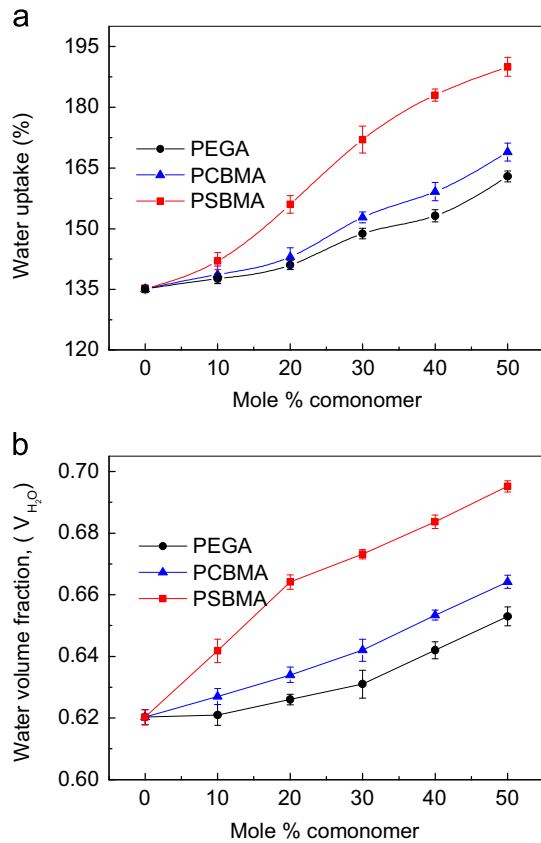


Fig. 4. Equilibrium pure water uptake (a) and water volume fraction (b) as functions of the co-monomer content.

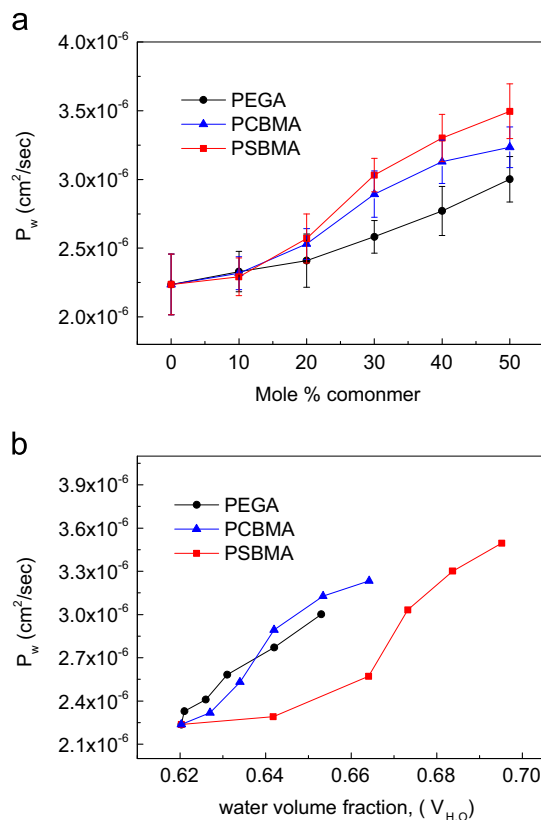


Fig. 5. Water permeability (calculate by Eq. (5)) as a function of co-monomer content (a) and water volume fraction (b).

the discussion for water uptake behavior also can be used to explain the permeation behavior. It is interesting, though, that the water uptake of PSBMA films are much higher than that of PCBMA films but the water permeability coefficients of the two films are very similar. This result might be due to stronger hydrogen bonding between sulfonate groups and water compared to the carboxylate groups. Stronger water-sulfonate group hydrogen bonding can decrease the mobility of water within the polymer, thus resulting in a water permeability that is closer to the value observed for PCBMA.

The correlation of the water permeation with water volume fraction is shown in Fig. 5(b). Water permeability increases with water volume fraction of PSBMA less strongly than that for PCBMA and PEGA films. This result further suggests stronger hydrogen bonding and lower water mobility in PSBMA compared to PCBMA and PEGA films. Regardless, water permeability shows the general trend of increasing with the water volume fraction for all the films, which is consistent with previous research [16].

3.3. Salt transport properties

Salt sorption and diffusivity were measured via kinetic desorption experiments with 0.85 mol L⁻¹ NaCl solution at 298 K. Fig. 6(a) shows that NaCl diffusivity in the cross-linked films increases similarly as co-monomer content increases for the three materials. The PSBMA films exhibit somewhat higher diffusivity than PCBMA film samples at the same zwitterionic co-monomer content. This result is consistent with a relationship between water uptake and salt diffusivity for a wide variety of polymers [14]. The salt sorption coefficients (K_s) (shown in Fig. 6(b)) generally increase with increasing co-monomer content. The zwitterionic films show higher salt sorption than uncharged PEGA films (uncharged). The difference increases when co-monomer content increases. By plotting K_s as a function of water uptake (Fig. 6(c)), we see this difference may be primarily due to the different water uptake properties of the three films.

According to eq. (8), P_s can be calculated as the product of measured D_s and K_s values. In Fig. 7, salt permeability of the films increases similarly with increasing co-monomer content as expected based on the increase of D_s and K_s with increasing co-monomer content. Due to the similar D_s values observed at each co-monomer composition, we believe that the different salt permeability values of three films mostly result from differences in salt sorption coefficients, K_s .

An approach used by Yasuda seeks to correlate salt diffusion with water content using free volume theory [16]. Similarly, we have correlated salt permeability with water sorption coefficients (Fig. 8), which can act as a proxy for free volume in swollen polymer systems [32]. The relationship between water content and salt permeability for zwitterionic polymers is generally consistent with Yasuda's model. High water sorption corresponds with high salt permeability. In addition, the zwitterionic film data cluster at the corner of high water sorption/high salt permeability suggesting that these materials may be too hydrophilic to be suitable for reverse osmosis applications that require relatively high levels of water/salt selectivity (i.e., high salt rejection). The high hydrophilicity, however, likely makes these materials attractive candidates for anti-fouling coatings. It is interesting that the slope of the data of zwitterionic polymers is different from Yasuda's slope. This might suggest that although zwitterionic polymers are overall neutral, the presence of positive and negative charged groups actually is contributing to excluding salt in some manner that is different from Yasuda's uncharged materials. This result may be similar to a result observed for charged sulfonated block copolymers [26].

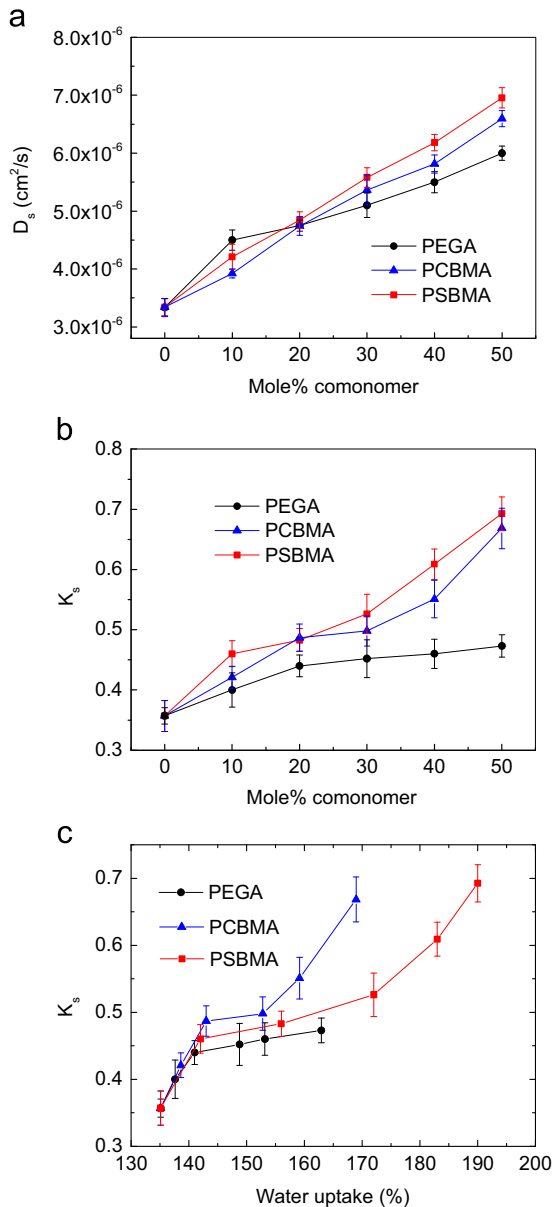


Fig. 6. Diffusion (a) and partition (b) coefficients of NaCl in polymer films as a function of composition as well as partition (c) coefficients of NaCl as a function of water uptake at 298 K with samples initially equilibrated in 0.85 M NaCl aqueous solution.

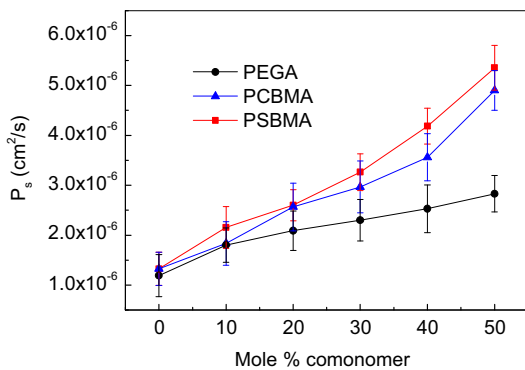


Fig. 7. Effect of monomer content on salt permeability of polymer films measured via kinetic desorption test at 298 K (with samples initially equilibrated in 0.85 M NaCl aqueous solution).

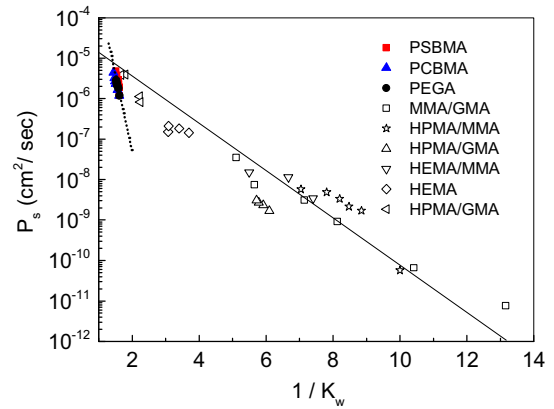


Fig. 8. Salt permeability (the product of the sodium chloride diffusion and sorption coefficient $D_s \times K_s = P_s$) versus the reciprocal water content of the hydrated polymer in DI water, compared to data published by Yasuda et al. [8]. The legend for copolymer data is shown as Table 1.

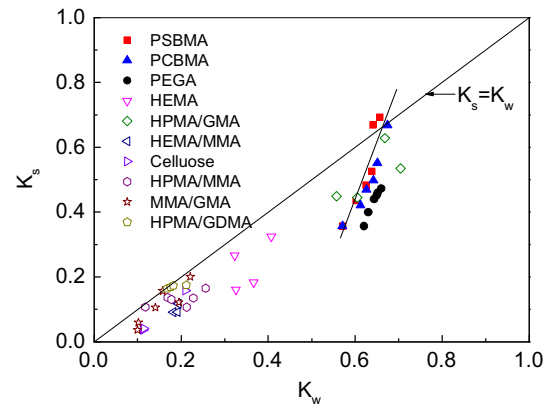


Fig. 9. Correlation of water content, K_w , and NaCl sorption coefficient, K_s , compared to data published by Yasuda et al. [8]. K_s was determined from kinetic desorption studies following equilibration in an aqueous salt solution at 298 K which contained 0.85 M NaCl, and K_w was measured in pure water. The legend for copolymer data is shown as Table 1.

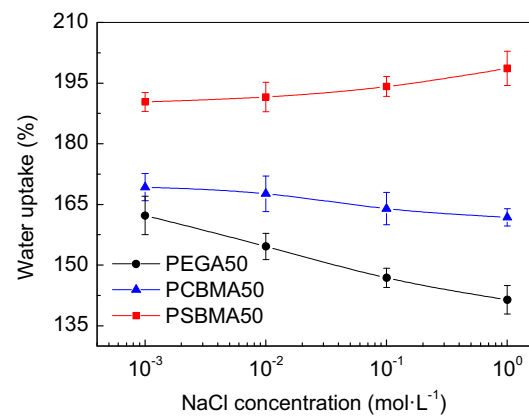


Fig. 10. Equilibrium water uptake for polymers soaked in NaCl solutions of different concentration.

Fig. 9 shows salt sorption coefficients as a function of the water sorption coefficient and compares the data measured in this study to data reported in the literature. The salt sorption coefficient represents the ratio of the concentration of NaCl in the polymer to the salt concentration in the solution in equilibrium with the polymer. Generally, K_s increases with K_w , which means that a polymer adsorbing more water will absorb more salt. The diagonal

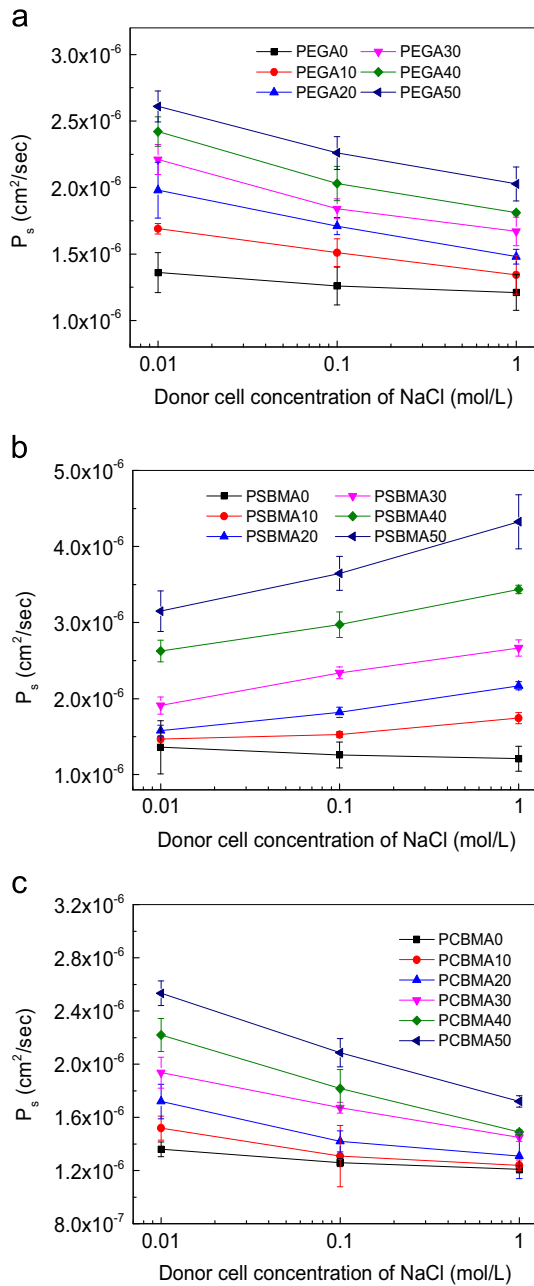


Fig. 11. Effect of donor NaCl concentration on salt permeability of (a) PEGA films, (b) PSBMA films and (c) PCBMA films measured with direct permeation cell at 298 K

solid line (Fig. 9) was plotted as $K_s = K_w$, i.e., the condition where the polymer would absorb water at the same salt concentration as the external solution (i.e., the polymer would not exclude salt from absorbing into the polymer) [13]. As shown in Fig. 9, most polymers have salt sorption coefficients that are lower than the water sorption coefficient meaning that these polymers exhibit some sorption selectivity for water compared to NaCl. By making a simple linear regression on data points of zwitterionic films, we also see that K_s drastically increase with K_w . The slope of the resulted line is higher than those of other polymers indicating that the K_s values of zwitterionic polymers may increase more rapidly with K_w than other polymers. This result may be related to electrostatic interactions between zwitterions and salt ions.

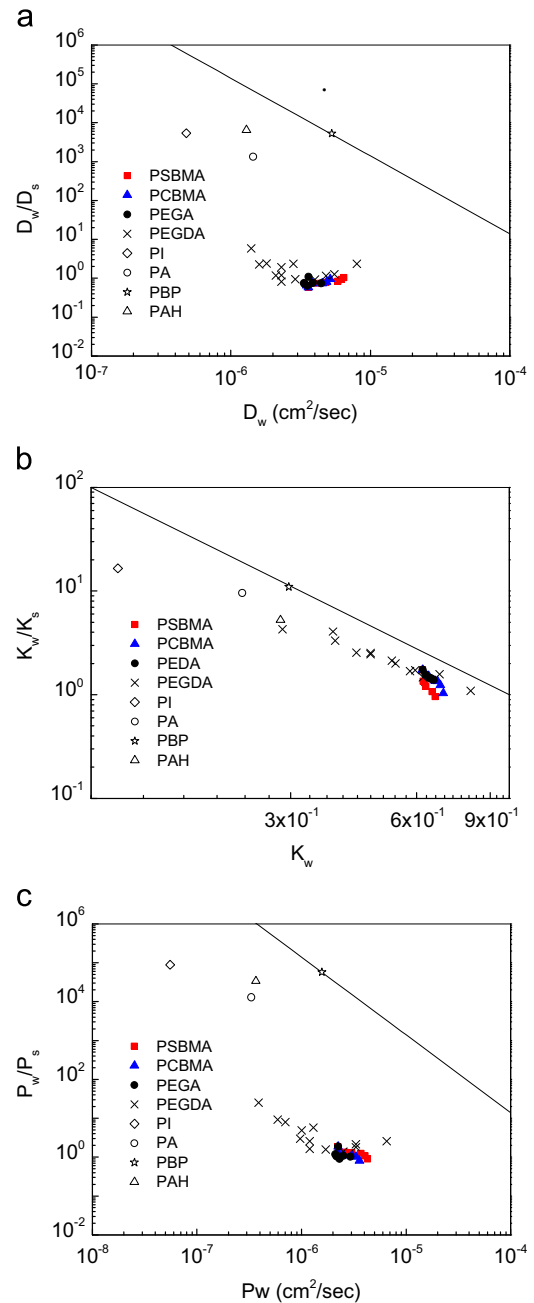


Fig. 12. Water/NaCl diffusivity selectivity as a function of water diffusivity in polymers film (a), water/NaCl sorption selectivity as a function of water partition coefficient in polymers film (b), and water/NaCl permeability selectivity as a function of diffusive water permeability in polymer films including PSBMA (■), PCBMA (▲), PEGA (●), XLPEGDA (×) = (crosslinked poly(ethylene glycol) [15], PI (◇) = polyimide [39], PA (○) = aromatic polyamide [39], PBP (☆) = polybenzimidazopyrrolone [39], PAH (△) = polyamide-hydrazide [39]). The line is the empirical tradeoff relationship reported in the literature [12].

3.4. Effect of salt concentration on transport properties

Charged and uncharged polymers have different salt transport property behavior when salt concentration is varied [13]. Herein, the salt concentration was varied to investigate its influence on the salt and water transport properties of the zwitterionic films. Fig. 10 shows the change in water uptake with surrounding salt concentration. The water uptake of PEGA and PCBMA films decreases with increasing NaCl concentration. This is consistent with previous research and is likely due to osmotic de-swelling [13].

Table 1
Legend for copolymer data shown in Fig. 9 and Fig. 10.

Symbol	Sample name
○	Hydroxyethyl methacrylate(HEMA) hydrogel
△	Hydroxypropyl methacrylate/glycerol methacrylate (HPMA/GMA) copolymer
▽	Hydroxyethyl methacrylate/methyl methacrylate(HEMA/MMA) copolymer
◁	Cellulose acetate %
▷	Methyl methacrylate/glycerol methacrylate(MMA/GMA) copolymer
◇	Methyl methacrylate/glycerol methacrylate(MMA/GMA) copolymer
□	Hydroxypropyl methacrylate/glycidyl methacrylate(HPMA/GdMA) copolymer

Strikingly, the water uptake of PSBMA increases with NaCl concentration. It is known that PSBMA swells to a greater extent at high salt concentrations [36]. This result is due to the “salt-in” effect where sulfonate groups tend to ionize, which can lead to suppression of interaction between zwitterions and scission of the crosslinking of zwitterions, which in turn, allows PSBMA to swell more freely. The carboxylate groups in PCBMA are only slightly deprotonated. The interactions between zwitterions, therefore, are weak, and the increase in water uptake due to increased salt concentration (“salt-in” effect) is overshadowed by osmotic de-swelling. Therefore, the water uptake of PCBMA slightly decreases with increasing NaCl concentration.

The effect of NaCl concentration on the NaCl permeability of the three polymer films are shown in Fig. 11. The decrease of the salt diffusion coefficients in the uncharged PEGA material can be understood as increased salt concentration reduces the water content and free volume of the hydrated polymer via osmotic de-swelling, and in turn, reduces diffusion coefficients and permeability coefficients [3]. In striking contrast to PEGA films, the salt permeability of PSBMA films increases as upstream external salt solution concentration increases, which is similar to behavior observed for sulfonated (charged) polymers [26]. As the concentration of salt increases in the external solution, the concentration of mobile salt absorbed in the polymer increases due to electrostatic screening of the charged groups within the polymer, resulting in increased NaCl sorption and permeability. Similarly, it has been reported that the salt diffusion coefficient of sulfonated polymers increase with external salt concentration [20]. In the PCBMA films, the effects of decreasing of free volume due to osmotic de-swelling may prevail over the effect of salt sorption increasing with external NaCl concentration. Therefore, PCBMA behaves more like an uncharged polymer film (i.e., behaves more like PEGA than PSBMA) due to its low charge density at the experimental pH. However, it should be noted here that PCBMA may show different salt concentration dependent transport behavior at low pH due to enhanced charge density then.

3.5. Water/salt selectivity

Water flux and salt rejection measurements, which are commonly used as metrics for characterizing polymers are highly sensitive to the measurement conditions used, but permeability selectivity, i.e., the ratio of water permeability to salt permeability can be used to characterize the intrinsic water/salt separation properties of polymers [12]. The ideal water/salt permeability selectivity, $\alpha_{w/s}$, can be defined as the ratio of water to salt permeability, and this value can then be related to sorption and diffusivity selectivity values (i.e., ratios of the water and salt sorption and diffusion coefficients) via the solution diffusion model, Eq. (8), [24]:

$$\alpha_{w/s} = \frac{P_w}{P_s} = \frac{K_w}{K_s} \times \frac{D_w}{D_s} \quad (11)$$

Fig. 12(a)–(c) shows tradeoff relationships between diffusion, sorption, and permeability selectivity and water diffusivity, sorption

and permeability, respectively. A trade-off relationship exists between water diffusivity, sorption and permeability and their corresponding selectivities. Similar trade-off relationships between permeability and selectivity are widely used in gas separation membrane research [37–39]. The solid lines shown in Fig. 12 have been developed empirically from data reported in the literature [12]. Polyamide-type polymer films (PA and PAH) exhibit high selectivity [40], while crosslinked poly (ethylene oxide) films (PEGDA) are highly water-swollen and show a low water/salt selectivity [15].

A similar tradeoff is also observed for PSBMA and PCBMA films as the transport data are clustered at the high permeability/low selectivity corner. For different polymer families, polymers with high water content tend to have high NaCl sorption and low water/NaCl sorption selectivity, further confirming the correlation of the polymer transport properties with water uptake. Among the data in Fig. 12, zwitterionic films exhibit high water permeability but low water/salt selectivity. Zwitterionic films are promising as coating materials for fouling control, but they may be less suitable for many desalting applications that require high water/salt selectivity (Table 1).

4. Conclusions

A series of zwitterionic polymer films were prepared by UV crosslinking of acrylate and methacrylate monomers and their salt/water transport properties were studied. Water and salt transport properties can be correlated with water uptake. Crosslink density strongly influences water uptake and water permeability of UV crosslinked films. Zwitterionic films exhibited similar water and salt transport property dependence on crosslink density. Water permeability increases as the crosslink density decreases, while salt permeability increases more rapidly, which is consistent with a free volume interpretation of water and salt transport in polymers. In addition, PSBMA and PCBMA salt permeability values vary differently with salt concentration. PSBMA behaves like a charged polymer, and its salt permeability increases with salt concentration. Alternatively, PCBMA behaves like an uncharged film and salt permeability decreases with increasing salt concentration. Similar to crosslinked PEG films, the zwitterionic polymer transport properties are consistent with a tradeoff between water permeability and water/salt selectivity. They are highly permeable and less selective polymers compared to other polymers reported in the literature. Zwitterionic polymers are attractive for use as coating layers for fouling control because of their water binding and foulant repellent properties, but low water/salt selectivity may limit their use as the sole desalting layer in a composite reverse osmosis membrane.

Acknowledgements

The authors gratefully acknowledge the financial support by The National Nature Science Foundation of China (Grant no.

21274108) and the National High Technology Research and Development Program of China (863 Program of China, 2012AA03A602). Prof. MJQ also thanks Prof. Benny Freeman and Mrs. Ni Yan (University of Texas at Austin, USA) for helpful discussions.

Appendix A. Supporting information

Supplementary data associated with this article can be found in the online version at <http://dx.doi.org/10.1016/j.memsci.2015.05.030>.

References

- [1] L.F. Greenlee, D.F. Lawler, B.D. Freeman, B. Marrot, P. Moulin, Reverse osmosis desalination: water sources, technology, and today's challenges, *Water Res.* 43 (2009) 2317–2348.
- [2] G.M. Geise, H.S. Lee, D.J. Miller, B.D. Freeman, J.E. McGrath, D.R. Paul, Water purification by membranes: the role of polymer science, *J. Polym. Sci., Part B: Polym. Phys.* 48 (2010) 1685–1718.
- [3] G.M. Geise, B.D. Freeman, D.R. Paul, Sodium chloride diffusion in sulfonated polymers for membrane applications, *J. Membr. Sci.* 427 (2013) 186–196.
- [4] Y.C. Chiang, Y. Chang, C.J. Chuang, R.C. Ruaan, A facile zwitterionization in the interfacial modification of low bio-fouling nanofiltration membranes, *J. Membr. Sci.* 389 (2012) 76–82.
- [5] Q.F. An, Y.L. Ji, W.S. Hung, K.R. Lee, C.J. Gao, AMOC positron annihilation study of zwitterionic nanofiltration membranes: correlation between fine structure and ultrahigh permeability, *Macromolecules* 46 (2013) 2228–2234.
- [6] Q.F. An, W.D. Sun, Q. Zhao, Y.L. Ji, C.J. Gao, Study on a novel nanofiltration membrane prepared by interfacial polymerization with zwitterionic amine monomers, *J. Membr. Sci.* 431 (2013) 171–179.
- [7] Y.L. Ji, Q.F. An, Q. Zhao, W.D. Sun, K.R. Lee, H.L. Chen, C.J. Gao, Novel composite nanofiltration membranes containing zwitterions with high permeate flux and improved anti-fouling performance, *J. Membr. Sci.* 390 (2012) 243–253.
- [8] R. Yang, H. Jang, R. Stocker, K.K. Gleason, Synergistic prevention of biofouling in seawater desalination by zwitterionic surfaces and low-level chlorination, *Adv. Mater.* 26 (2014) 1711–1718.
- [9] D.R. Paul, Reformulation of the solution-diffusion theory of reverse osmosis, *J. Membr. Sci.* 241 (2004) 371–386.
- [10] J.G. Wijmans, R.W. Baker, The solution-diffusion model: a review, *J. Membr. Sci.* 107 (1995) 1–21.
- [11] H.K. Lonsdale, U. Merten, R.L. Riley, Transport properties of cellulose acetate osmotic membranes, *J. Appl. Polym. Sci.* 9 (1965) 1341–1362.
- [12] G.M. Geise, H.B. Park, A.C. Sagle, B.D. Freeman, J.E. McGrath, Water permeability and water/salt selectivity tradeoff in polymers for desalination, *J. Membr. Sci.* 369 (2011) 130–138.
- [13] G.M. Geise, D.R. Paul, B.D. Freeman, Fundamental water and salt transport properties of polymeric materials, *Prog. Polym. Sci.* 39 (2014) 1–42.
- [14] H. Yasuda, C.E. Lamaze, L.D. Ikenberry, Permeability of solutes through hydrated polymer membranes. Part I. Diffusion of sodium chloride, *Die Makromol. Chem.* 118 (1968) 19–35.
- [15] H. Ju, A.C. Sagle, B.D. Freeman, J.I. Mardel, A.J. Hill, Characterization of sodium chloride and water transport in crosslinked poly(ethylene oxide) hydrogels, *J. Membr. Sci.* 358 (2010) 131–141.
- [16] A.C. Sagle, H. Ju, B.D. Freeman, M.M. Sharma, PEG-based hydrogel membrane coatings, *Polymer* 50 (2009) 756–766.
- [17] H. Ju, B.D. McCloskey, A.C. Sagle, Y.H. Wu, V.A. Kusuma, B.D. Freeman, Cross-linked poly(ethylene oxide) fouling resistant coating materials for oil/water separation, *J. Membr. Sci.* 307 (2008) 260–267.
- [18] X. Gong, A. Bandis, A. Tao, G. Meresi, Y. Wang, P.T. Inglefield, A.A. Jones, W. Y. Wen, Self-diffusion of water, ethanol and decafluoropentane in perfluoro-sulfonate ionomer by pulse field gradient NMR, *Polymer* 42 (2001) 6485–6492.
- [19] M.A. Hickner, Ion-containing polymers: new energy & clean water, *Mater. Today* 13 (2010) 34–41.
- [20] G.M. Geise, L.P. Falcon, B.D. Freeman, D.R. Paul, Sodium chloride sorption in sulfonated polymers for membrane applications, *J. Membr. Sci.*, 423, 2012195–208.
- [21] F.G. Donnan, The theory of membrane equilibria, *Chem. Rev.* 1 (1924) 73–90.
- [22] W. Pusch, Measurement techniques of transport through membranes, *Desalination* 59 (1986) 105–198.
- [23] Z. Zhang, S.F. Chen, S.Y. Jiang, Dual-functional biomimetic materials: Nonfouling poly(carboxybetaine) with active functional groups for protein immobilization, *Biomacromolecules* 7 (2006) 3311–3315.
- [24] W. Xie, J. Cook, H.B. Park, B.D. Freeman, C.H. Lee, J.E. McGrath, Fundamental salt and water transport properties in directly copolymerized disulfonated poly(arylene ether sulfone) random copolymers, *Polymer* 52 (2011) 2032–2043.
- [25] A.C. Sagle, E.M. Van Wagner, H. Ju, B.D. McCloskey, B.D. Freeman, M. M. Sharma, PEG-coated reverse osmosis membranes: desalination properties and fouling resistance, *J. Membr. Sci.* 340 (2009) 92–108.
- [26] G.M. Geise, B.D. Freeman, D.R. Paul, Characterization of a sulfonated pentablock copolymer for desalination applications, *Polymer* 51 (2010) 5815–5822.
- [27] M.L. Huggins, Thermodynamic properties of solutions of long-chain compounds, *Ann. N.Y. Acad. Sci.* 43 (1942) 1–32.
- [28] P.J. Flory, Thermodynamics of high polymer solutions, *J. Chem. Phys.* 10 (2004) 51–61.
- [29] H. Ju, B.D. McCloskey, A.C. Sagle, V.A. Kusuma, B.D. Freeman, Preparation and characterization of crosslinked poly(ethylene glycol) diacrylate hydrogels as fouling-resistant membrane coating materials, *J. Membr. Sci.* 330 (2009) 180–188.
- [30] F.G. Helfferich, Ion exchange, New York: Courier Dover Publications, 1995.
- [31] Q. Shao, S. Jiang, Molecular understanding and design of zwitterionic materials, *Adv. Mater.* 27 (2015) 15–26.
- [32] W. Xie, H. Ju, G.M. Geise, B.D. Freeman, J.I. Mardel, A.J. Hill, J.E. McGrath, Effect of free volume on water and salt transport properties in directly copolymerized disulfonated poly(arylene ether sulfone) random copolymers, *Macromolecules* 44 (2011) 4428–4438.
- [33] V. Tandon, S.K. Bhagavatula, W.C. Nelson, B.J. Kirby, zeta potential and electroosmotic mobility in microfluidic devices fabricated from hydrophobic polymers: 1. The origins of charge, *Electrophoresis* 29 (2008) 1092–1101.
- [34] V. Tandon, B.J. Kirby, Zeta potential and electroosmotic mobility in microfluidic devices fabricated from hydrophobic polymers: 2. Slip and interfacial water structure, *Electrophoresis* 29 (2008) 1102–1114.
- [35] S.H. Goh, Y. Liu, S.Y. Lee, C.H.A. Huan, Miscibility and interactions in blends and complexes of poly(N-acryloyl-N'-phenylpiperazine) with acidic polymers, *Macromolecules* 32 (1999) 8595–8602.
- [36] Q. Yang, M. Ulbricht, Novel membrane adsorbers with grafted zwitterionic polymers synthesized by surface-initiated ATRP and their salt-modulated permeability and protein binding properties, *Chem. Mater.* 24 (2012) 2943–2951.
- [37] L.M. Robeson, Correlation of separation factor versus permeability for polymeric membranes, *J. Membr. Sci.* 62 (1991) 165–185.
- [38] L.M. Robeson, W.F. Burgoyne, M. Langsam, A.C. Savoca, C.F. Tien, High performance polymers for membrane separation, *Polymer* 35 (1994) 4970–4978.
- [39] B.D. Freeman, Basis of permeability/selectivity tradeoff relations in polymeric gas separation membranes, *Macromolecules* 32 (1999) 375–380.
- [40] W.J. Koros, G.K. Fleming, S.M. Jordan, T.H. Kim, H.H. Hoehn, Polymeric membrane materials for solution-diffusion based permeation separations, *Prog. Polym. Sci.* 13 (1988) 339–401.